THE ASTROPHYSICAL JOURNAL, 407:402–411, 1993 April 10

ION ABUNDANCES AND IMPLICATIONS FOR PHOTOCHEMISTRY IN COMETS HALLEY (1986 III) AND BRADFIELD (1987 XXIX)

BARRY L. LUTZ AND MARIA WOMACK
Department of Physics and Astronomy, Box 6010, Northern Arizona University, Flagstaff, AZ 86011

AND

R. MARK WAGNER
Department of Astronomy, Ohio State University, Columbus, OH 43210
Received 1992 July 7; accepted 1992 October 1

ABSTRACT

Spectra of the plasma tails of comets P/Halley (1986 III) and P/Bradfield (1987 XXIX, also 1987s) were recorded using the Ohio State University Image Dissector Scanner (IDS) on the Perkins 1.8 m telescope at the Lowell Observatory. The ionic species CO^+, N_2^+, CH^+, and H_2O^+ were identified in these spectra and column densities for them were calculated from measured fluxes. The observed abundance ratios of CO^+/H_2O^+ in comets Halley and Bradfield are consistent with predictions by photochemical models, provided that CO^+ and H_2O^+ are produced primarily from photoionization of CO and H_2O, respectively. However, the observed N_2^+/H_2O^+ ratios are at least an order of magnitude lower and the observed CH^+/H_2O^+ ratios are a factor of 100 higher, than theoretical results. The abundance ratio N_2/CO was derived in the plasma tail of Bradfield from N_2^+ and CO^+ data, and found to be an order of magnitude higher than a value measured in Halley. The relative ion abundances of CH^+, N_2^+, CO^+ and H_2O^+ in Halley are consistent with in situ measurements obtained from the *Giotto* spacecraft. Fluorescence efficiencies have been recalculated for optical transitions of N_2^+, CH^+, NH, CH, OH^+, and CO and are also presented.

Subject headings: comets, individual (Halley, Bradfield) — molecular processes

1. INTRODUCTION

One of the most prominent features in a comet is an extensive (10^{5-7} km) plasma tail which usually develops at close heliocentric distances and points radially away from the Sun. The plasma tail arises from a complex interaction of cometary ions with the interplanetary magnetic field carried by solar wind particles. It may exhibit such structures as kinks, knots, and disconnections. Understanding the physics and chemistry of molecular ions within the tail is critical for understanding the dynamics and composition of cometary comae.

A general description of a cometary atmosphere has been developed from numerous observations of recent bright comets, including data obtained from the *Giotto*, *Vega* and *ICE* spacecraft encounters (e.g., Schmidt et al. 1988; Huebner et al. 1991). At ~ 1 AU from the Sun, a coma can be divided into four distinct zones. Within a few thousand km of the nucleus, the coma is considered to be a neutral gas of molecules free of solar wind particles and bounded by a "contact surface." Outside the contact surface is a region of relatively free expansion of pure cometary plasma bounded at $\sim 1 \times 10^5$ km by a "cometopause," a pileup of magnetic field lines which divide a predominantly cometary gas from a predominantly solar wind (Gringauz et al. 1986). The coma perimeter is generally thought to extend to $\sim 10^6$ km where a bow shock is created, separating a cometary hydrogen plasma and solar wind mixture from pure solar wind.

Different chemical and physical conditions characterize each zone in a cometary atmosphere. For example, the gas densities are high enough only in the inner region ($< 10^5$ km) for significant chemistry to occur and most of the coma ions are thought to form in this region through gas-phase ion-molecule chemical reactions and photoionization (Huebner & Giguere 1980). Farther out, the densities are insufficient for most chemical reactions to occur, with the exception of photodissociation and photoionization of tail ions.

The differing chemistry affects the molecular and ionic abundances in a coma, which can, in principle, be measured from ground-based observations. In particular, knowledge of the relative abundances of key ionic species as a function of time and radial distance from the nucleus may be used to investigate the production and destruction of ions and neutrals in the comet gas. Molecular ion abundances also have the potential to yield insight to the development of a cometary plasma and its interaction with the solar wind (e.g., Ip & Mendis 1976; Huebner & Giguere 1980; Schmidt et al. 1988).

With the exception of the *Giotto*, *Vega* and *ICE* spacecraft data, very few observations of molecular ions in a cometary plasma have been published. The CO^+/H_2O^+ abundance ratio has been measured in a few comets and found to be approximately unity (e.g., Debi Prasad, Jockers, & Geyer 1992; Wagner, Lutz, & Wyckoff 1987; Lutz 1987). However, observations of other cometary molecular ions, such as N_2^+ and CH^+, have been only rarely reported. Both comets Halley and Bradfield developed prominent ion tails and presented an excellent opportunity to study the physical and chemical behavior of the ions N_2^+, CH^+, CO^+, and H_2O^+. In this paper, we present optical spectra and column densities of these species in the plasma tails of comets Halley and Bradfield and compare the results with predictions of photochemical models. For Halley, the ion abundances are also compared with in situ measurements from the various mass spectrometer experiments carried by the *Giotto* spacecraft.

2. OBSERVATIONS

We obtained spectra of comet Bradfield during 1987 November 23–December 23 and of comet Halley during 1985

TABLE 1

SUMMARY OF COMET OBSERVATIONS

Comet	UT Date	r (AU)	Δ (AU)	ρ_A (km)
Bradfield.....	1987 Nov 23.4	0.91	0.91	4224
	1987 Nov 24.1	0.92	0.91	4224
	1987 Nov 25.1	0.93	0.91	4224
	1987 Dec 9.1	1.00	0.84	3900
	1987 Dec 23.1	1.20	0.87	4038
Halley.....	1985 Dec 13.1	1.30	0.79	3680
	1985 Dec 14.2	1.28	0.80	3710

TABLE 2

OBSERVED MOLECULAR IONS IN COMETS

Species	Transition	λ (Å)
N_2^+	B–X (0–0)	3914
CO^+	A–X (4–0)	3787
	A–X (3–0)	4010
	A–X (2–0)	4260
	A–X (1–0)	4553
CH^+	A–X (0–0)	4235
H_2O^+	A–X (8–0)	6153

December 13–14 using the Ohio State University Image Dissector Scanner (Byard et al. 1981) on the Perkins 1.8 m telescope of the Ohio State University at the Lowell Observatory. The dual beam circular entrance apertures of the spectrograph projected to 6.″4 ($\rho_A \sim 4000$ km) in diameter on the plane of the sky and were separated by 39″ center–center. A 600 lines mm^{-1} grating blazed at 5500 Å was employed covering the wavelength region 3750–6350 Å with a spectral resolution of ~ 10 Å. A summary of the observations is listed in Table 1. A list of cometary ions observed is given in Table 2. The position angle (P.A.) of the plasma tail on the plane of the sky, measured north through east, is given in Table 3 for each spectrum. Precise offsetting was achieved by using the telescope pointing software, and careful guiding was performed by monitoring the bright nuclear condensation on the slit-viewing TV acquisition system.

Sky removal was performed by subtracting spectra of the night sky obtained 2.°5 from the comet from each comet spectrum. A close solar analog star, van Bueren 64 (Hardorp 1982), was observed with the same instrumental configuration as the comet and was used to remove the reflected solar continuum from cometary spectra. Continuum bandpasses were chosen based on observations of other comets (e.g., Wagner et al. 1987), and continuum fluxes were measured in both the comet and solar analog spectra. The spectrum of the solar analog star was then scaled to the cometary continuum fluxes and subtracted from the comet spectrum.

In order to avoid excessive contamination of the N_2^+ (0–0) band by C_3 emission, and the H_2O^+ (8–0) band by C_2 ($\Delta v = -2$) emission, we confined the observations of the plasma tail of comet Bradfield to points 2×10^4, 3×10^4, and 6×10^4 km downstream from the bright nuclear condensation. Spectra of comet Halley were obtained at tailward offsets of 1×10^4, 2×10^4, 2×10^5, and 3×10^5 km from the nucleus. In addition, we recorded spectra of comets Bradfield and Halley at an offset of 2×10^4 km on the sunward side of the comae.

3. RESULTS

Spectra of comet Bradfield's plasma tail taken at a distance of 2×10^4 and 6×10^4 km from the nuclear condensation on 1987 November 25 are presented in Figure 1. Ion spectra of comet Halley obtained at 2×10^4 and 2×10^5 km tailward offsets on 1985 December 13 are shown in Figure 2. The positions of the N_2^+ (0–0), CO^+, (4–0), (3–0), (2–0), (1–0), H_2O^+, (8–0) bands are indicated. As the figures show, CO^+ was relatively strong in Bradfield, but not observed in the Halley spectra presented here. On the other hand, H_2O^+ appears stronger in Halley. N_2^+ was conclusively identified only in comet Bradfield at 6×10^4 km tailward on 1987 November 24, 25, and December 23. CH^+ was observed on one night each in Halley and Bradfield at 2×10^4 km tailward. Emission band fluxes were extracted for the N_2^+ (0–0), CH^+ (0–0), CO^+ (2–0), and H_2O^+ (8–0) bands and are given in Table 3. Observed temporal and spatial variations in the cometary ions are discussed in the following section.

4. DISCUSSION

4.1. *Ion Column Densities*

Electronic transitions of cometary ions are excited by resonance fluorescence, so that the column density of an ion, N, is

TABLE 3

OBSERVED FLUXES OF COMETARY IONS

COMET	UT DATE	AIR MASS	OFFSET (km)	P.A.	F_λ (ergs cm^{-2} s^{-1}) N_2^+	CH^+	CO^+	H_2O^+
Bradfield	1987 Nov 23	1.5	2×10^4	238°	$<4.6 \times 10^{-14}$	$<5.2 \times 10^{-15}$	$(3.0 \pm 0.6) \times 10^{-14}$	$(1.4 \pm 0.3) \times 10^{-13}$
	1987 Nov 24	1.5	2×10^4	58	$<1.5 \times 10^{-13}$	$<1.2 \times 10^{-14}$	$(1.2 \pm 0.2) \times 10^{-13}$	$<1.5 \times 10^{-13}$
	1987 Nov 24	1.5	6×10^4	58	$(5.1 \pm 1.0) \times 10^{-14}$	$<1.4 \times 10^{-14}$	$(7.0 \pm 1.4) \times 10^{-14}$	$<6.9 \times 10^{-14}$
	1987 Nov 25	1.5	2×10^4	58	$<8.7 \times 10^{-14}$	$(1.5 \pm 0.3) \times 10^{-14}$	$(2.0 \pm 0.4) \times 10^{-13}$	$(1.1 \pm 0.2) \times 10^{-13}$
	1987 Nov 25	1.5	6×10^4	58	$(7.1 \pm 1.4) \times 10^{-14}$	$<1.7 \times 10^{-14}$	$(1.3 \pm 0.3) \times 10^{-13}$	$(6.2 \pm 0.2) \times 10^{-14}$
	1987 Dec 9	1.8	3×10^4	90	$<1.0 \times 10^{-13}$	$<3.0 \times 10^{-14}$	$(7.8 \pm 1.6) \times 10^{-14}$	$<2.5 \times 10^{-13}$
	1987 Dec 9	1.8	6×10^4	56	$<2.7 \times 10^{-14}$	$<1.4 \times 10^{-14}$	$(1.1 \pm 0.2) \times 10^{-13}$	$<1.1 \times 10^{-13}$
	1987 Dec 23	1.3	6×10^4	58	$(2.1 \pm 0.4) \times 10^{-14}$	$<4.8 \times 10^{-15}$	$(3.8 \pm 0.8) \times 10^{-14}$	$<5.8 \times 10^{-14}$
Halley	1985 Dec 13	1.4	2×10^4	217	$<1.5 \times 10^{-13}$	$<3.3 \times 10^{-14}$	$<4.0 \times 10^{-14}$	$(4.3 \pm 0.9) \times 10^{-13}$
	1985 Dec 13	1.3	1×10^4	90	$<1.5 \times 10^{-13}$	$<3.2 \times 10^{-14}$	$<2.4 \times 10^{-14}$	$(1.2 \pm 0.2) \times 10^{-13}$
	1985 Dec 13	1.2	2×10^4	37	$<1.5 \times 10^{-13}$	$(3.0 \pm 0.6) \times 10^{-14}$	$(3.9 \pm 0.8) \times 10^{-14}$	$(1.2 \pm 0.2) \times 10^{-13}$
	1985 Dec 13	1.6	2×10^5	70	$<3.7 \times 10^{-14}$	$<1.1 \times 10^{-15}$	$<1.2 \times 10^{-14}$	$(4.7 \pm 1.0) \times 10^{-14}$
	1985 Dec 13	1.8	3×10^5	70	$<8.8 \times 10^{-15}$	$<3.8 \times 10^{-15}$	$<9.9 \times 10^{-15}$	$(3.7 \pm 0.7) \times 10^{-14}$
	1985 Dec 14	1.8	2×10^4	249	$<1.8 \times 10^{-13}$	$<2.8 \times 10^{-14}$	$<7.5 \times 10^{-14}$	$(9.6 \pm 1.9) \times 10^{-14}$
	1985 Dec 14	1.9	2×10^4	90	$<8.3 \times 10^{-14}$	$<1.9 \times 10^{-14}$	$(3.7 \pm 0.7) \times 10^{-14}$	$(1.0 \pm 0.2) \times 10^{-13}$

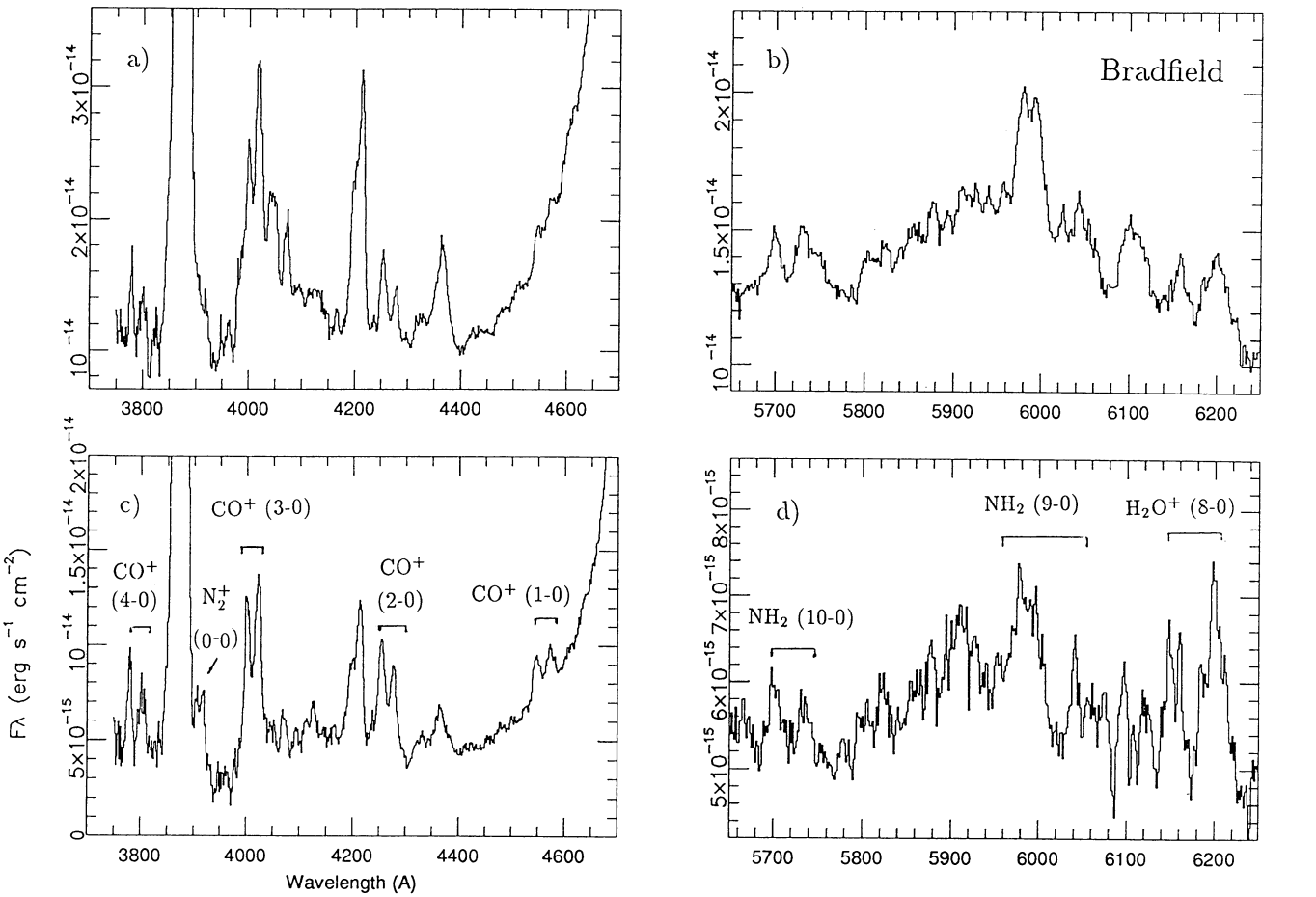

FIG. 1.—Spectra of comet Bradfield on 1987 November 25 at (*a*) and (*b*) 2 × 10^4 km tailward and (*c*) and (*d*) 6 × 10^4 km tailward

given by

$$N = \frac{4\pi F}{\Omega g}, \qquad (1)$$

where F is the integrated molecular band flux, Ω is the solid angle subtended by the spectrograph slit at the comet and g is the fluorescence efficiency, or g-factor, of the molecule. Fluorescence efficiencies at 1 AU of 3.6 × 10^{-3} photons s^{-1} for the CO^+ (2–0) transition (Magnani & A'Hearn 1986), and 4.2 × 10^{-3} photons s^{-1} ion^{-1} for the H_2O^+ (8–0) (Lutz 1987) band have been adopted. Fluorescence efficiencies for N_2^+ and CH^+ have been recalculated in the Appendix. In all cases, g-factors were scaled to the appropriate heliocentric distance, r(AU), according to $g(r) = g(1\text{ AU})/r^2$.

Column densities of N_2^+, CH^+, CO^+, and H_2O^+ were calculated for comets Halley and Bradfield and are presented in Table 4. For Kohoutek, we recalculated the N_2^+ and CH^+ column densities using the band luminosities presented by Wyckoff & Wehinger (1976) and the newly determined fluorescence efficiencies for these ions listed in the Appendix. The new CH^+ column density is ~70% larger and the N_2^+ column density is ~30% larger than the original calculations of Wyckoff & Wehinger (1976), based on the old fluorescence efficiencies of N_2^+ and CH^+. The H_2O^+ column density for Kohoutek was taken from Lutz (1987), where it was recomputed from the original Kohoutek band intensities and recently recalculated H_2O^+ g-factors. The estimated uncertainty for the column densities of N_2^+, CO^+, and H_2O^+ is ~30%, while those for CH^+ are a little higher, ~50%, due to a less certain CH^+ fluorescence efficiency.

Temporal variability was apparent in most of the ion column densities in comet Bradfield. For example, N_2^+, CO^+, and H_2O^+ emission increased by $\gtrsim$50% from 1987 November 24–25, followed by a factor of 2 decrease in abundance during November 25–December 9. This variability is slightly greater than photometric measurements of Bradfield which indicate that the comet varied in brightness up to 30% on a daily basis during 1987 November–December (D. G. Schleicher 1992, private communication). No temporal variability greater than 30% was observed in cometary ions of Halley, however. Narrow-band photometry of comet Halley indicates that the comet's production of C_2 (an indicator of overall comet brightness) decreased by ~25% between December 13 and 14 (Schleicher et al. 1990). However, this decrease is smaller than the uncertainties of the column density calculations and, hence, could not be detected in the data presented here.

Spatial variation in the column densities of a few ions was observed in comet Halley. For example, on December 13 the column density of H_2O^+ was observed to drop by at least a factor of 5 from 2 × 10^4 km to 2 × 10^5 km in the tail. This decrease is well reproduced by several photochemical models which predict the ion's abundance to fall by a factor of ~5–8 over that distance (e.g., Huebner et al. 1991; Biermann,

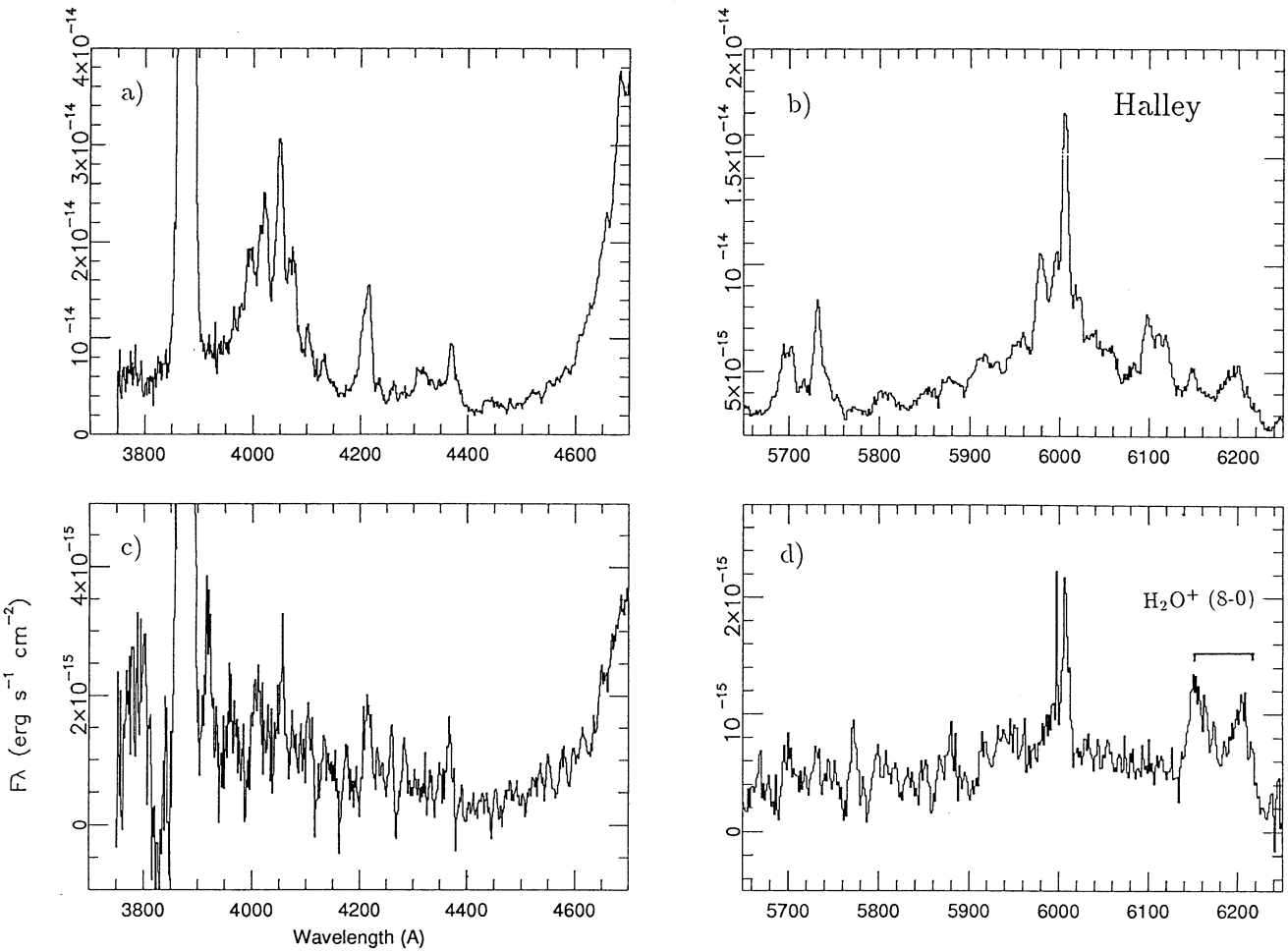

FIG. 2.—Spectra of comet Halley on 1985 December 13 at (*a*) and (*b*) 2 × 10^4 km tailward and (*c*) and (*d*) 2 × 10^5 km tailward

Giguere, & Huebner 1982). No significant spatial variation (>30%) in ion column densities was observed from 2 × 10^4 km sunward to 6 × 10^4 km tailward in comet Bradfield. Additionally, no variation in ion abundances was measured in sunward versus tailward positions for either comet.

4.2. *Halley: A Comparison with the Giotto Results*

The results of two experiments on *Giotto* have been published: (1) the heavy ion analyzer, RPA2-PICCA, by Korth et al. (1987), and (2) the IMS-HERS analyzer by Balsiger et al. (1987). The PICCA was designed to determine the composition and energy distributions of thermal, positively charged ions while the HERS was intended to study primarily the interaction region of the solar wind with cometary ions. As is seen in Table 5, the HERS instrument measured relative abundance ratios of the ions CO^+ and N_2^+ (both indistinguishable at 28 amu) with H_2O^+ (at 18 amu) which ranged from ~0.5 to ~0.9 between 5 × 10^4 and 2 × 10^5 km sunward, respectively. The PICCA instrument measured $(N_2^+ + CO^+)/H_2O^+ \sim 0.3$ at only one position, 2 × 10^3 km on the sunward side. The single ground-based measurement of the ratio which we obtained at 2 × 10^4 km tailward on 1985 December 14 yields a ratio of $(N_2^+ + CO^+)/H_2O^+ = 0.2 \pm 0.1$. Our ground-based ratio is close to the HERS measurement of 0.5 ± 0.1 obtained at 5 × 10^4 km sunward and very near the ratio of 0.3 deduced from the PICCA measurement at 2 × 10^3 km sunward. However, we note that most the PICCA measurement was obtained within the contact surface of the coma, a region which is thought to have a chemistry very different from the comae at 2 × 10^4 km. Upper limits to the ratio which we obtained at other tailward positions in comet Halley had an average value of $(N_2^+ + CO^+)/H_2O^+ < 0.3$, which is at least a factor of 2 lower than the HERS sunward results. The upper limit of <0.5 which we derived from our single sunward observation at 2 × 10^4 km is consistent with the HERS ratio of ~0.5 at 5 × 10^4 km.

Measurements at 13 amu on the HERS instrument from 50,000 to 140,000 km on the sunward side have been attributed to CH^+ (Balsiger et al. 1986) and yield an abundance ratio of $CH^+/H_2O^+ \sim 0.01$, as denoted in Table 5. The *Giotto* result is consistent with our ground-based measurement of $CH^+/H_2O^+ = 0.03 \pm 0.02$ obtained at 20,000 km on the tailward side.

The comparisons should be interpreted with caution for several reasons. First, the ground-based measurements are ratios of column densities in which the ion mass densities are effectively integrated through a column passing through a point on the plasma tail, while the spacecraft results refer to actual densities measured along the path of *Giotto*. Second, the *Giotto* results were obtained on the sunward side of the

TABLE 4

COLUMN DENSITIES OF COMETARY IONS

COMET	UT DATE	OFFSET (km)	N (ions cm^{-2}) N_2^+	CH^+	CO^+	H_2O^+
Bradfield	1987 Nov 23	2×10^4 sunward	$<7.2 \times 10^9$	$<2.0 \times 10^{10}$	$(9.8 \pm 2.9) \times 10^{10}$	$(6.0 \pm 1.8) \times 10^{11}$
	1987 Nov 24	2×10^4 tailward	$<2.4 \times 10^{10}$	$<2.0 \times 10^{10}$	$(4.0 \pm 1.2) \times 10^{11}$	$<3.6 \times 10^{11}$
	1987 Nov 24	6×10^4 tailward	$(7.3 \pm 2.2) \times 10^9$	$<5.4 \times 10^{10}$	$(2.4 \pm 0.7) \times 10^{11}$	$<1.7 \times 10^{11}$
	1987 Nov 25	2×10^4 tailward	$<1.4 \times 10^{10}$	$(6.1 \pm 3.0) \times 10^{10}$	$(6.9 \pm 2.1) \times 10^{11}$	$(4.9 \pm 1.5) \times 10^{11}$
	1987 Nov 25	6×10^4 tailward	$(1.2 \pm 0.4) \times 10^{10}$	$<6.5 \times 10^{10}$	$(4.5 \pm 1.3) \times 10^{11}$	$(2.8 \pm 0.8) \times 10^{11}$
	1987 Dec 9	3×10^4 tailward	$<2.0 \times 10^{10}$	$<1.4 \times 10^{11}$	$(3.1 \pm 0.9) \times 10^{11}$	$<3.2 \times 10^{11}$
	1987 Dec 9	6×10^4 tailward	$<5.0 \times 10^9$	$<6.4 \times 10^{10}$	$(4.4 \pm 1.3) \times 10^{11}$	$<3.0 \times 10^{11}$
	1987 Dec 23	6×10^4 tailward	$(5.7 \pm 1.7) \times 10^9$	$<3.2 \times 10^{11}$	$(2.2 \pm 0.6) \times 10^{11}$	$<4.3 \times 10^{11}$
Halley	1985 Dec 13	2×10^4 sunward	$<1.6 \times 10^{11}$	$<1.2 \times 10^{10}$	$<3.2 \times 10^{11}$	$(1.2 \pm 0.3) \times 10^{12}$
	1985 Dec 13	1×10^4 tailward	$<6.0 \times 10^{10}$	$<5.9 \times 10^{10}$	$<2.3 \times 10^{11}$	$(9.6 \pm 2.9) \times 10^{11}$
	1985 Dec 13	2×10^4 tailward	$<1.3 \times 10^{10}$	$(6.0 \pm 3.0) \times 10^{10}$	$(2.6 \pm 0.8) \times 10^{11}$	$(2.1 \pm 0.6) \times 10^{12}$
	1985 Dec 13	2×10^5 tailward	$<1.2 \times 10^{10}$	$<9.4 \times 10^9$	$<8.0 \times 10^{10}$	$(4.1 \pm 1.2) \times 10^{11}$
	1985 Dec 13	3×10^5 tailward	$<2.8 \times 10^9$	$<3.2 \times 10^9$	$<6.6 \times 10^{10}$	$(3.2 \pm 1.0) \times 10^{11}$
	1985 Dec 14	2×10^4 sunward	$<5.5 \times 10^{10}$	$<2.3 \times 10^{10}$	$<4.9 \times 10^{11}$	$(8.1 \pm 2.4) \times 10^{11}$
	1985 Dec 14	2×10^4 tailward	$<2.5 \times 10^{10}$	$<1.6 \times 10^{10}$	$(2.4 \pm 0.7) \times 10^{11}$	$(8.4 \pm 2.5) \times 10^{11}$

nucleus, while the ground-based ratios were obtained in the plasma tail. Third, the ground-based measurements are preperihelion while the *Giotto* results are postperihelion. Nevertheless, there is no large discrepancy between the results, giving added support to the measurements.

4.3. *Comparison with Models of Ion Behavior*

In order to probe ion behavior in the coma, we intercompared the abundances of ionic species as a function of radial distance from the comet. The ratios of the column densities of N_2^+, CH^+, and CO^+ with respect to H_2O^+ are summarized for Halley and Bradfield in Table 6. Abundance ratios for comets Kohoutek, Giacobini-Zinner, and Wilson are included for comparison. Predictions from photochemical models of cometary comae are also listed in Table 6.

The relative abundances of CO^+ and H_2O^+ are thought to depend critically on the chemistry of the parent molecules and have been the subject of considerable study in photochemical modeling of cometary atmospheres (see Huebner 1985; Schmidt et al. 1988). While it is generally assumed that H_2O^+ is formed primarily from photoionization of H_2O (e.g., Huebner & Giguere 1980; Biermann et al. 1982; Huebner et al. 1991), CO^+ may not derive from a single, dominant parent molecule in a cometary atmosphere. In the innermost coma, $<1 \times 10^3$ km from the nucleus, most models assume that CO^+ is produced by photodissociative ionization of CO-bearing molecules, such as

$$h\nu + CO_2 \rightarrow O + CO^+ + e\,. \quad (2)$$

On the other hand, in the intermediate coma ($\sim 10^{4-5}$ km), CO^+ is thought to form by photoionization of CO,

$$h\nu + CO \rightarrow CO^+ + e \quad (3)$$

(e.g., Huebner 1985). With CO_2 as the parent molecule, the CO^+/H_2O^+ ratio at $\lesssim 1 \times 10^4$ km in the tail is predicted to be ~ 0.05. With CO as the parent, the models predict a much larger ratio, ranging from $CO^+/H_2O^+ \sim 0.4$ at 1×10^4 km to ~ 0.6 at 1×10^5 km in the plasma tail (e.g., Huebner & Giguere 1980).

All of the observed CO^+/H_2O^+ ratios presented here were measured between 1×10^4 and 3×10^5 km in the plasma tails and are the same order of magnitude as predictions by models which assume that CO rather than a CO_2 is the parent to CO^+. For example, the CO^+/H_2O^+ abundance ratio for comets Bradfield, Kohoutek, Wilson, and Giacobini-Zinner is on the order of unity, although the measurements for Halley are generally lower, $CO^+/H_2O^+ \sim 0.3$. Thus, the observations of CO^+ and H_2O^+ in comets Halley, Bradfield, Kohoutek, Wilson, and Giacobini-Zinner are consistent with a model in which H_2O^+ and CO^+ are produced by photoionization of H_2O and CO, respectively.

Very few model predictions exist for the abundances of N_2^+ and CH^+. Photochemical models predict the relative abundances of N_2^+ and H_2O^+ to range from $N_2^+/H_2O^+ \sim 0.4$ at 1×10^4 km to ~ 1.0 at 1×10^5 km (Biermann et al. 1982). Only two measurements were obtained for N_2^+/H_2O^+ in the comets. In Bradfield and Kohoutek, $N_2^+/H_2O^+ \sim 0.04$ and an upper limit of <0.1 was found for Halley. Thus, it appears that

TABLE 5

SUMMARY OF ABUNDANCE RATIOS IN COMET HALLEY

Source	Location	$(CO^+ + N_2^+)/H_2O^+$	CH^+/H_2O^+	Reference
Ground-based	2×10^4 sunward	<0.5	<0.01	This work
	1×10^4 tailward	<0.3	<0.06	This work
	2×10^4 tailward	0.2 ± 0.1	0.03 ± 0.02	This work
	2×10^5 tailward	<0.2	<0.02	This work
	3×10^5 tailward	<0.2	<0.01	This work
Giotto, IMS-HERS	5.3×10^4 sunward	0.5 ± 0.1	0.016 ± 0.020	Balsiger et al. 1987
	9.0×10^4 sunward	0.8 ± 0.2	0.015 ± 0.020	Balsiger et al. 1987
	1.4×10^5 sunward	0.9 ± 0.4	0.008 ± 0.005	Balsiger et al. 1987

TABLE 6

RELATIVE ABUNDANCES OF COMETARY IONS

Comet	Date	Location (km)	N_2^+/H_2O^+	CH^+/H_2O^+	CO^+/H_2O^+
Bradfield	1987 Nov 23	2×10^4 sunward	...	...	0.2 ± 0.1
	1987 Nov 24	2×10^4 tailward	...	...	>0.6
	1987 Nov 24	6×10^4 tailward	>0.04	...	>0.8
	1987 Nov 25	2×10^4 tailward	<0.03	0.12 ± 0.09	1.4 ± 0.7
	1987 Nov 25	6×10^4 tailward	0.04 ± 0.03	<0.23	1.6 ± 0.7
	1987 Dec 9	3×10^4 tailward	...	...	>0.2
	1987 Dec 9	6×10^4 tailward	...	...	>0.8
	1987 Dec 23	6×10^4 tailward	>0.01	...	>0.5
Halley	1985 Dec 13	2×10^4 sunward	<0.13	<0.01	<0.5
	1985 Dec 13	1×10^4 tailward	<0.06	<0.06	<0.2
	1985 Dec 13	2×10^4 tailward	<0.01	0.03 ± 0.02	0.2 ± 0.1
	1985 Dec 13	2×10^5 tailward	<0.03	<0.02	<0.2
	1985 Dec 13	3×10^5 tailward	<0.01	<0.01	<0.2
	1985 Dec 14	2×10^4 sunward	<0.07	<0.03	<0.6
	1985 Dec 14	2×10^4 tailward	<0.03	<0.02	0.3 ± 0.2
Giacobini-Zinner	1985 Sep 9, 12[a]	1×10^4 tailward	...	...	0.8 ± 0.7
Kohoutek[b,c,d]	1974 Jan 18	1×10^4 tailward	0.04 ± 0.03	0.09 ± 0.07	1.2 ± 0.4
Wilson[e]	1987 Apr 29	5×10^4 tailward	...	...	0.6
		1.5×10^5 tailward	...	...	0.6
Theoretical	...	6×10^3 tailward	...	0.0002[f]	...
(CO Parent)	...	1×10^4 tailward	0.36[g]	...	0.38[h]
(CO Parent)	...	2×10^4 tailward	0.44[g]	...	0.42[h]
(CO Parent)	...	1×10^5 tailward	0.96[g]	...	0.56[h]
(CO_2 Parent)	...	$<1 \times 10^4$ tailward	...	...	0.05[h]

[a] Wagner, Lutz, & Wyckoff 1987.
[b] Wyckoff & Wehinger 1976.
[c] Lutz 1987.
[d] This work.
[e] Debi Prasad, Jockers, & Geyer 1992.
[f] Wegmann et al. 1987.
[g] Biermann et al. 1982.
[h] Huebner & Giguere 1980.

model calculations of N_2^+ abundance may be too high by an order of magnitude.

The CH^+/H_2O^+ abundance ratio was observed to be 0.12 ± 0.08 in Bradfield, 0.03 ± 0.02 in Halley and 0.09 ± 0.06 in Kohoutek at $\sim 10^4$ km in the tail of each comet. Chemical modeling of the CH^+ cometary abundance outside the contact surface has been published in only one instance, $CH^+/H_2O^+ \sim 0.0002$ at 6000 km in the plasma tail (Wegmann et al. 1987), and is approximately 100 times lower than the ground-based and spacecraft results.

Another abundance ratio of interest is that of N_2^+ with respect to CO^+. These two ions are among the most stable against photodissociation and photoionization in a cometary atmosphere. Additionally, the most likely parent molecules of N_2^+ and CO^+, N_2 and CO respectively, have photoionization branching ratios of $\sim 50\%$ (Engel & Wyckoff 1993). In contrast, virtually all other molecular species observed in comets have photoionization branching ratios of only a few percent. Therefore, N_2^+ and CO^+ are expected to exhibit similar chemical behaviors in plasma tails. Additionally, once rate coefficients are known, observations of N_2^+ and CO^+ can be used to derive relative abundances of N_2 and CO, which are thought to be two of the most stable and dominant volatiles in a comet nucleus (e.g., Womack, Wyckoff, & Ziurys 1992). An average abundance ratio of $N_2/CO \sim N_2^+/CO^+ = 0.02 \pm 0.01$ was calculated for comet Bradfield at 6×10^4 km tailward on November 24 and 25, and December 9 and 23. No significant temporal variation was detected from the four nights, and data were available only at the 6×10^4 km position.

The derived N_2/CO abundance ratios at 6×10^4 km in Bradfield's plasma tail presented here are about an order of magnitude larger than the value calculated for 3×10^5 km in Halley's tail on 1986 Apr 10.54 UT under the same assumptions (Womack et al. 1992). Since N_2^+ and CO^+ are thought to be produced and destroyed in similar manners, models predict that the N_2^+/CO^+ abundance ratio is constant out to at least 4×10^5 km in the plasma tail (e.g., Biermann et al. 1982). Hence, this difference cannot be explained by chemical effects of the two ions at different positions in the tail. One possible explanation for the different N_2^+/CO^+ ratios is that Bradfield's nucleus may have contained more N_2 than Halley. Alternatively, Halley may have had more CO in its nucleus. It should be noted that Bradfield is a long-period comet ($1/a \sim 0.006368$; Marsden & Williams 1992), while Halley is considered a short-period comet. It is possible that Halley's nucleus (which presumably has had more passes by the Sun than Bradfield) may have had the original relative abundances of its volatiles altered compared to a Bradfield.

5. CONCLUSIONS

Column densities of CO^+, H_2O^+, N_2^+, and CH^+ were calculated from optical spectra of the plasma tails of comets Halley and Bradfield. Comparison of the observed relative abundances of CO^+ and H_2O^+ with photochemical models indicate that in the intermediate (10^{4-5} km) region of comae, the two ions are most probably produced via photoionization of CO and H_2O. Current cometary models do not reproduce the observed relative abundances of N_2^+ and CH^+ with respect to H_2O^+. Theoretical calculations appear to overproduce N_2^+ by a factor of ~ 10, while underproducing CH^+ by up to two orders of magnitude. An abundance ratio of N_2/CO in comet

Bradfield was calculated from N_2^+ and CO^+ data and found to be an order of magnitude larger than the same ratio observed previously in comet Halley, which suggests that the two comets may have had different thermal or chemical histories.

The authors thank S. Willard III who helped in the early stages of data reduction. B. L. and M. W. acknowledge grant NAGW-2811, from the Planetary Astronomy Program of the National Aeronautics and Space Administration.

APPENDIX

REVISED FLUORESCENCE EFFICIENCY FACTORS FOR N_2^+, CO, C_2, CH^+, NH, OH^+, AND CH

Conversion of measured fluxes to column densities for each of the observed optical transitions within the model of fluorescent scattering of solar radiation requires fluorescence efficiency factors, given by (e.g., Chamberlain & Hunten 1987),

$$g_{v'v''} = \pi F_\odot \lambda_{v'v''}^2 f_{v'v''} \left(\frac{\pi e^2}{mc^2}\right) \frac{A_{v'v''}}{\Sigma_{v''} A_{v'v''}}, \quad (4)$$

where $\pi F_\odot$ is the incident solar flux, $\lambda_{v'v''}$ is the wavelength of the band origin, $f_{v'v''}$ is the band oscillator strength, $A_{v'v''}/\Sigma_{v'} A_{v'v''}$ is the branching ratio for downward transitions into the observed band, and $(\pi e^2/mc^2) = 8.23 \times 10^{-21}$ cm^2 Å^{-1}, if $\lambda_{v'v''}$ is in units of Å, and other values are expressed in cgs units. We have recomputed fluorescence efficiencies for N_2^+, CO, C_2, CH^+, NH, OH^+, and CH at 1 AU using this formalism, the approximations and techniques described by Lutz (1987), and the Neckel & Labs (1984) solar irradiances. The results of these calculations are presented in this Appendix and its associated tables.

For the $B\,^2\Sigma_u^+ - X\,^2\Sigma_g^+$ system of N_2^+, a lifetime of 60.5 ns (Dotchin, Chupp, & Pegg 1973; Huber & Herzberg 1979) was adopted for the B state, and the Franck-Condon factors for the B–X transition were taken from Lofthus & Krupenie (1977). Table 7 summarizes the derived g-factors for the (0–0) and (1–0) bands. The close packing of the rotational fine structure in molecules such as N_2^+ minimizes any Swings effects on the g-factors for integrated bands, as is indicated by Hsu & Smith (1977). Based on uncertainties in the measured lifetime, Franck-Condon factors and solar irradiances we estimate the total uncertainties to be about $\pm 20\%$ for the larger values of $g_{v'v''}$ associated with the Franck-Condon parabola. Increased uncertainties are expected in the smaller values primarily due to increased uncertainties for Franck-Condon factors off the Franck-Condon parabola.

For CO, fluorescence efficiencies have been calculated for the $B\,^1\Sigma^+$–$X\,^1\Sigma^+$ and $B\,^1\Sigma$–$A\,^1\Pi$ systems. The g-factors for the B–X system were computed assuming that the electronic branching ratios of 0.68 for the B–X transition and 0.32 for B–A, and that the lifetime of the B state was 23 ns (Dotchin et al. 1973). Franck-Condon factors were computed by Carlson et al. (1978). The g-factors for the CO B–X system are listed in Table 8, while those for $B-A$ are in Table 9. The uncertainties for these g-factors are probably on the order of $\pm 50\%$ given the large uncertainties of the solar uv flux and its known variables.

TABLE 7

BAND ORIGINS AND FLUORESCENCE EFFICIENCY FACTORS FOR N_2^+ $B\,^2\Sigma_u^+$–$X\,^2\Sigma_g^+$ SYSTEM[a]

	v''							
v'	0	1	2	3	4	5	6	7
0.....	3910	4274	4705	5224	5860	6659	7690	9073
	7.0(−2)	2.2(−2)	4.3(−3)	7.2(−4)	9.6(−5)	2.2(−5)	*	*
1.....	3578	3880	4232	4647	5144	5750	6503	7465
	9.0(−3)	5.1(−3)	5.2(−3)	1.9(−3)	4.4(−4)	8.7(−5)	1.5(−5)	3.3(−6)

[a] In each matrix cell, the upper number is the vacuum wavelength of the band origin of the fluorescing transition in Å, computed from molecular parameters; the lower number is the fluorescence efficiency factor in photons s^{-1} ion^{-1}, at 1 AU. The numbers in parentheses are powers of 10. An asterisk signifies that Franck-Condon factors were negligible for a particular transition.

TABLE 8

BAND ORIGINS AND FLUORESCENCE EFFICIENCY FACTORS FOR CO $B\,^1\Sigma^+$–$X\,^1\Sigma^+$ SYSTEM[a]

	v''		
v'	0	1	2
0.....	1150	1179	1209
	4.6(−10)	4.7(−12)	4.9(−13)
1.....	1123	1151	1180
	2.7(−13)	2.5(−11)	*

[a] See note to Table 7.

TABLE 9

BAND ORIGINS AND FLUORESCENCE EFFICIENCY FACTORS FOR CO $B\,^1\Sigma^+$–$A\,^1\Pi$ SYSTEM[a]

	v''				
v'	0	1	2	3	4
0.....	4510	4832	5194	5602	6065
	3.3(−11)	5.6(−11)	5.3(−11)	3.7(−11)	2.1(−11)

[a] See note to Table 7.

TABLE 10

BAND ORIGINS AND FLUORESCENCE EFFICIENCY FACTORS FOR C_2 $A\,^1\Pi$–$X\,^1\Sigma^+$ SYSTEM[a]

	v''				
v'	0	1	2	3	4
0.....	12091	15523	21552	34906	89574
	4.7(−2)	2.1(−2)	3.1(−3)	1.5(−4)	9.5(−7)
1.....	10147	12459	16065	22474	37023
	3.9(−2)	3.4(−4)	8.4(−3)	2.9(−3)	2.1(−4)
2.....	8760	10431	12845	16639	23466
	1.1(−2)	7.1(−3)	1.3(−3)	1.2(−3)	1.1(−3)
3.....	7721	8990	10728	13252	17248
	2.1(−03)	4.1(−3)	3.8(−4)	9.2(−4)	5.3(−5)
4.....	6914	7914	9231	11039	13680
	2.6(−4)	1.0(−3)	7.1(−4)	3.6(−6)	2.5(−4)
5.....	6269	7080	8116	9482	11366
	3.1(−5)	1.9(−4)	3.0(−4)	1.0(−4)	2.7(−5)
6.....	5742	6416	7254	8326	9745
	3.6(−6)	3.0(−5)	8.2(−5)	6.8(−5)	3.2(−6)

[a] See note to Table 7.

Fluorescence efficiencies calculated for the $A\,^1\Pi$–$X\,^1\Sigma^+$ transitions of C_2 are based on an assumed lifetime of 16,000 ns for the A state (Davis et al. 1984) and Franck-Condon factors computed by Dwivedi et al. (1978). The C_2 g-factors are listed in Table 10 and the uncertainties are probably about $\pm 25\%$, since the solar flux in this region is relatively smooth and any Swings effect is unlikely.

For the CH^+ $A\,^1\Pi$–$X\,^1\Sigma^+$ system, the lifetime of the A state is not a constant with vibrational level, indicative of the breakdown of the Born-Oppenheimer approximation (Yoshimine, Green, & Thaddeus 1973; Elander, Oddershede, & Beebe 1977). To correct for the insufficiency of the Born-Oppenheimer approximation, we adopted a different radiative lifetime for each vibrational level along with the Franck-Condon factors published by Green, Horstein, & Bender (1973). The adopted lifetimes are those measured by Erman (1977; see also Huber & Herzberg 1979) and are 630, 750, and 850 ns for the $v = 0$, 1, and 2 levels respectively. The g-factors for these CH^+ emissions are listed in Table 11.

Because of the large rotational constants associated with a hydride such as CH^+, fluorescence by these molecules is susceptible to variations in g-factors due to the Swings effect on each of the contributing line in the band. In all cases the lifetimes have uncertainties of about $\pm 10\%$, while the Franck-Condon factors are probably better than $\pm 10\%$ for the stronger bands. The additional errors due to the application of the Born-Oppenheimer approximation and to the Swings effect are more difficult to evaluate, but we believe that with these uncertainties included, our g-factors for CH^+ should be accurate to within $\pm 50\%$.

For the NH $A\,^3\Pi$–$X\,^3\Sigma^-$ system, a lifetime of 404 ns for the A state (Huber & Herzberg 1979) was adopted, and the Franck-Condon factors were taken from Smith & Liszt (1971). In Table 12 are summarized the derived g-factors. Like CH^+, NH transitions are susceptible to the Swings effect. Consequently the uncertainty in these g-factors may be as high as $\pm 50\%$.

TABLE 11

BAND ORIGINS AND FLUORESCENCE EFFICIENCY FACTORS FOR CH^+ $A\,^1\Pi$–$X\,^1\Sigma^+$ SYSTEM[a]

	v''						
v'	0	1	2	3	4	5	6
0.....	4235	4790	5478	6348	7480	9005	11161
	2.8(−2)	7.7(−3)	1.2(−3)	1.1(−4)	7.7(−6)	4.4(−6)	*
1.....	3961	4443	5028	5751	6665	7850	9439
	2.9(−3)	1.4(−3)	1.9(−3)	6.7(−4)	1.2(−4)	1.9(−5)	*
2.....	3752	4182	4697	5322	6095	7071	8336
	3.1(−4)	9.3(−4)	*	2.9(−4)	3.0(−4)	4.2(−5)	9.1(−5)

[a] See note to Table 7.

TABLE 12

BAND ORIGINS AND FLUORESCENCE EFFICIENCY FACTORS FOR NH $A\,^3\Pi$–$X\,^3\Sigma$-SYSTEM[a]

	v''		
v'	0	1	2
0.....	3357	3751	4221
	1.3(−2)	1.9(−6)	1.3(−7)
1.....	3047	3368	3742
	3.3(−10)	1.2(−6)	2.3(−9)
2.....	2804	3074	3383
	1.7(−12)	1.2(−10)	3.4(−8)

[a] See note to Table 7.

TABLE 13

BAND ORIGINS AND FLUORESCENCE EFFICIENCY FACTORS FOR OH^+ $A\,^3\Pi$–$X\,^3\Sigma^-$ SYSTEM[a]

	v″						
v′	0	1	2	3	4	5	6
0.....	3577	4000	4505	5114	5858	6784	7956
	1.3(−3)	4.7(−4)	6.6(−5)	4.4(−6)	*	*	*
1.....	3341	3707	4137	4644	5251	5982	6875
	3.4(−4)	1.4(−4)	2.7(−4)	8.0(−5)	9.3(−6)	4.5(−7)	*
2.....	3150	3473	3848	4283	4794	5396	6112
	2.9(−5)	7.1(−5)	2.0(−7)	4.4(−5)	2.8(−5)	5.2(−6)	3.5(−7)
3.....	2994	3284	3617	3999	4441	4953	5550
	2.3(−6)	1.2(−5)	7.1(−6)	2.4(−6)	4.4(−6)	7.4(−6)	2.6(−6)

[a] See note to Table 7.

For the OH^+ $A\,^3\Pi$–$X\,^3\Sigma^-$ system, a lifetime of 2500 ns for the A state was taken from Mohlmann et al. (1978) and the Franck-Condon factors were from de Almeida & Singh (1981). In Table 13 are summarized the derived g-factors. Again, we estimate an uncertainty of $\pm 50\%$, primarily due to possible Swings effects.

Fluorescence efficiencies were also calculated for the $A\,^2\Delta$–$X\,^2\Pi_r$, $B\,^2\Sigma^-$–$X\,^2\Pi_r$, and $C\,^2\Sigma^+$–$X\,^2\Pi_r$ transitions of CH. The lifetimes of the A and B states, 534 and 380 ns, respectively, were taken from Huber & Herzberg (1979), and Franck-Condon factors were taken from McCallum, Jarmain, & Nichols (1970). The fluorescence efficiencies for A–X and B–X systems are given in Tables 14 and 15, respectively. For the C state, a lifetime of 120 ns was computed from $f(0\text{–}0) = 6 \times 10^{-3}$ (see Huber & Herzberg 1979). A g-factor was calculated for only the (0–0) transition at 3146 Å, since its Franck-Condon factor is ~ 0.999, and found to be 5.6×10^{-3} mol s^{-1}. The total uncertainty in these values for CH may be also as large as $\pm 50\%$.

TABLE 14

BAND ORIGINS AND FLUORESCENCE EFFICIENCY FACTORS FOR CH $A\,^2\Delta$–$X\,^2\Pi_r$ SYSTEM[a]

	v″			
v′	0	1	2	3
0.....	4306	4880	5592	6492
	2.2(−2)	1.2(−4)	1.0(−5)	*
1.....	3852	4305	4849	5512
	1.6(−6)	1.3(−4)	9.1(−7)	1.2(−7)

[a] See note to Table 7.

TABLE 15

BAND ORIGINS AND FLUORESCENCE EFFICIENCY FACTORS FOR CH $B\,^2\Sigma^-$–$X\,^2\Pi_r$ SYSTEM[a]

	v″										
v′	0	1	2	3	4	5	6	7	8	9	10
0.....	3890	4353	4910	5592	6439	7519	8931	10845	13569	17714	24711
	6.9(−3)	6.5(−4)	7.9(−5)	*	*	*	*	*	*	*	*
1.....	3637	4038	4513	5082	5773	6626	7699	9081	10915	13447	17128
	1.7(−4)	5.9(−4)	1.3(−4)	6.0(−5)	3.2(−6)	3.5(−6)	*	1.8(−7)	*	*	*
2.....	3469	3832	4257	4760	5361	6089	6983	8101	9530	11405	13948
	1.0(−6)	2.5(−5)	1.3(−5)	7.6(−6)	1.2(−5)	2.8(−6)	2.5(−6)	4.5(−7)	3.2(−7)	3.9(−8)	2.4(−8)

[a] See note to Table 7.

REFERENCES

Balsiger, H., et al. 1986, Nature, 321, 330
Balsiger, H., et al. 1987, A&A, 187, 163
Biermann, L., Giguere, P. T., & Huebner, W. F. 1982, A&A, 108, 221
Boice, D. C., Huebner, W. F., Sablik, M. J., & Konno, I. 1990, Geoph. Res. Lett., 17, 1813
Byard, P. L., Foltz, C. B., Jenkner, H., & Peterson, B. M. 1981, PASP, 93, 147
Carlson, T. A., Duric, N., Erman, P., & Larsson, M. 1978, Z. Phys. A, 123
Chamberlain, J. W., & Hunten, D. 1987, in Theory of Planetary Atmospheres (2d ed.; Orlando: Academic) 290
Davis, S. P., Smith, W. H., Brault, J. W., Pecyner, R., & Wagner, J. 1984, ApJ, 287, 455
de Almeida, A. A., & Singh, P. D. 1981, A&A, 95, 383
Debi Prasad, C., Jockers, K., & Geyer, E. H. 1992, Icarus, 95, 211
Dotchin, L. W., Chupp, E. L., & Pegg, D. J. 1973, J. Chem. Phys., 59, 3960
Dwivedi, P. H., Branch, D., Huffaker, J. N., & Bell, R. A. 1978, ApJS, 36, 573
Elander, N., Oddershede, J., & Beebe, N. H. F. 1977, ApJ, 216, 165
Engel, L. R., & Wyckoff, S. 1993, in preparation
Erman, P. 1977, ApJ, 213, L89
Green, S., Horstein, S., & Benden, C. F. 1973, ApJ, 179, 671
Gringauz, K. I., et al. 1986, Geophys. Res. Lett., 13, 613
Hardorp, J. 1982, A&A, 105, 120
Hsu, D. K., & Smith, W. H. 1977, J. Chem. Phys., 66, 1835
Huber, K. P., & Herzberg, G. 1979, Constants of Diatomic Molecules (New York: Van Nostrand Reinhold)
Huebner, W. F. 1985, in The Photochemistry of Atmospheres: Earth, the Other Planets, and Comets, ed. J. S. Levine (Orlando: Academic), 438

Huebner, W. F., Boice, D. C., Schmidt, H. U., & Wegmann, R. 1991, in Comets in the Post-Halley Era, ed. R. L. Newburn, M. Neugebauer, & J. Rahe (Dordrecht: Kluwer), 907
Huebner, W. F., & Giguere, P. T. 1980, ApJ, 238, 753
Ip, W.-H., & Mendis, D. A. 1977, Icarus, 30, 377
Korth, A., et al. 1987, A&A, 187, 149
Lofthus, A., & Krupenie, P. H. 1977, J. Phys. Chem. Ref. Data, 6, 113
Lutz, B. L. 1987, ApJ, 315, L47
Magnani, L., & A'Hearn, M. F. 1986, ApJ, 302, 477
Marsden, B. G., & Williams, G. V. 1992, in Catalog of Cometary Orbits (Cambridge MA: IAU Central Bureau for Astronomical Telegrams) 95
McCallum, J. C., Jarmain, W. R., & Nicholls, R. W. 1970, Spec. Rept. 1, York Univ.
Mohlman, G. R., Bhutani, K. K., de Heer, F. J., & Tsurubuchi, S. 1978, Chem. Phys., 31, 273
Neckel, H., & Labs, D. 1984, Sol. Phys, 232, 374
Schleicher, D. G., et al. 1990, AJ, 100, 896
Schmidt, H. U., Wegmann, R., Huebner, W. F., & Boice, D. C. 1988, Comput. Phys. Comm., 49, 17
Smith, W. H., & Liszt, H. S. 1971, J. Quant. Spectrosc. Rad. Transf., 11, 45
Wagner, R. M., Lutz, B. L., & Wyckoff, S. 1987, ApJ, 322, 544
Wegmann, R., Schmidt, H. U., Huebner, W. F., & Boice, D. C. 1987, A&A, 187, 339
Womack, M., Wyckoff, S., & Ziurys, L. M. 1992, ApJ, 401, 728
Wyckoff, S., & Wehinger, P. A. 1976, ApJ, 204, 604
Yoshimine, M., Green, S., & Thaddeus, P. 1973, ApJ, 183, 899